Effects of Surface-Immobilization on Photobleaching of Xanthene Dye Photocatalysts

Sarah Freeburne,[a] Jessica L. Sacco,[a] Esther W. Gomez,[a] Christian W. Pester[b]

[a] Department of Chemical Engineering, The Pennsylvania State University
[b] Department of Chemical Engineering, Department of Chemistry, Department of Materials Science and Engineering, The Pennsylvania State University, 314 CBEB, University Park, PA 16802, USA
E-mail: pester@psu.edu

Keywords: Photocatalysis, Photobleaching

ABSTRACT

While organic photocatalysts provide increasingly versatile chemical pathways under mild conditions, their long-term stability remains understudied. Here, the photobleaching behavior of xanthene dye photocatalysts is investigated. Rose Bengal, Eosin Y, and fluorescein are studied when in solution, when grafted to glass beads, and when incorporated into polymer brushes that are tethered to glass beads. This provides a comparison between Xanthene's stability as a homogeneous and as a heterogeneous photocatalyst. Photobleaching was investigated using UV-Vis, diffuse reflectance UV-Vis (DR UV-VIS), and fluorescence microscopy. Xanthene dyes as homogeneous photocatalysts exhibited the highest photostability, while the grafted systems appeared to fade more rapidly. Notably, heterogenization appeared to have different effects based on the photocatalyst system, and further altering the photocatalyst environment with reagents may improve stability.

Introduction

In light of the global concerns for sustainability and energy efficiency, photocatalysis has captured increasing interest.[1–3] Photocatalysis offers the ability to enable or accelerate the rate of a chemical reaction using mild visible light as a stimulus at ambient temperatures and pressures. This approach is promising for the reduction of energy demands in industrial synthesis, as electric LEDs or even natural sunlight have proven useful options.

Organic photocatalysis have received increasing interest as they are naturally higher in abundance, in contrast to the effective, but expensive, iridium and ruthenium-based photocatalysts.[4,5] Some key requirements in the design and functioning of photocatalysts

include sufficiently long excited state lifetimes, broad absorption, and compatible redox capabilities. [6,7] The wavelengths of usable light for photocatalysis can be tailored and depends on the photocatalyst itself, with wavelengths spanning from ~280 nm to 980 nm having been reported. [8,9]

While the design parameters for photocatalysts have received scientific attention, there is less detailed and limited information on the photostability (or photobleaching) and longevity of these photocatalysts. Photobleaching is the process of photocatalyst deactivation, in which the catalyst is no longer able to absorb light and facilitate chemical transformations. While studies have been performed in context of biological labelling and imaging,[10] more studies are needed in order to determine the photobleaching behavior and impact in photocatalytic settings. Past work has determined the bleaching kinetics of Erythrosin B,[11] fluorescein,[12,13] and Eosin Y,[14] for example, but these studies involve harsher settings than required for photocatalysis by using conditions such as high intensity laser irradiation or aqueous environments which may accelerate catalyst oxidation and degradation.

Specifically for the design of recyclable heterogeneous photocatalysts,[15–17] knowledge on photobleaching rates after surface-immobilization becomes essential for photocatalyst selection. Heterogeneous photocatalysts exist in a phase different from the reactants, which facilitates recovery and recycling to offer ecological and economic benefits. Consequently, with recovery and reuse after a chemical reaction as the goal, the long-term stability and behavior of immobilized photocatalysts becomes even more vital.

Here, we focus on the study of xanthene dyes as a model photocatalyst class and compare the photostability of three different derivatives in solution, grafted directly to glass beads as monolayers, and incorporated within polymer chains tethered to glass surfaces. Such heterogenized xanthene photocatalysts immobilized on nanoparticles,[18] glass/silica beads,[19] and glass wool[20] have been of interest recently. Both the xanthene monolayer[18,20] and the xanthene polymer brush[21,22] approach have been used successfully as heterogeneous photocatalysts tethered to various solid supports. However, the effects of surface-functionalization on photobleaching have not been studied. Some reports have suggested that photocatalysts may become more resilient to photobleaching when immobilized on nanoparticles.[18,23] The stability of photocatalysts on larger micron-scale supports, however, remain unexplored. Potential consequences of larger supports include lower surface area to

volume ratios, which can result in lower photocatalytic efficiency from limitations on catalyst loadings. Lower relative (local) photocatalyst concentrations may alter the catalyst stability, as self-quenching of photocatalysts, or quenching by oxygen may have a more significant effect on catalyst stability.

Results and Discussion

This study focuses on the stability of fluorescein, Eosin Y, and Rose Bengal as homogeneous catalysts and when immobilized onto solid supports. Fluorescein has been shown useful to catalyze e.g., cyclic condensation reactions,[24] photoinduced electron transfer reversible addition fragmentation chain transfer polymerization (PET-RAFT),[21] and degradation of pollutants, such as the antibiotic tetracycline.[25] Eosin Y can catalyze PET-RAFT polymerizations,[26] atom transfer radical polymerization (ATRP),[27] and other reactions such as the oxidative cleavage of styrene.[28] Rose Bengal has been shown to catalyze e.g., dehydrogenative and cycloaddition reactions.[29] **Table 1** shows the measured molar absorptivity for the three dyes studied herein.

Table 1. Comparison of molar extinction coefficients ε (L mol^{-1} cm^{-1}), calculated using concentration calibration curves for both the maximum value within 350 to 600 nm, as well as for 525 nm, corresponding to the maximum emission of the green LED lights. Coefficients were determined in DMSO solvent.

Photocatalyst	ε_{max} / (L mol^{-1} cm^{-1})	ε_{max} (525nm) / (L mol^{-1} cm^{-1})
Fluorescein	40,000	37,000
Eosin Y	104,000	37,000
Rose Bengal	83,500	20,500

For photobleaching studies, dimethyl sulfoxide (DMSO) was selected as the solvent due to its common use with xanthene-based photocatalysts. DMSO also acts as an active quencher of singlet oxygen, offering the benefit of oxygen tolerance in radical reactions.[30] This O_2-tolerance also allows for the study of the photocatalysts in photosensitization environments while mitigating the risks of oxidation.[31]

Photobleaching of xanthene dye solutions in DMSO

To evaluate photobleaching, time-resolved UV-Vis spectroscopy was used to measure changes in absorbance over time. Each photocatalyst was monitored for a decline in the maximum peak signal intensity (Eosin Y: λ_{max} = 538 nm; fluorescein: λ_{max} = 521 nm; Rose Bengal: λ_{max} = 565 nm). Declining absorbance indicates changes in active photocatalyst concentrations, and lower

absorbance over time indicates potential photocatalyst degradation or photobleaching, which results in a reduced catalytic potential. Green LEDs (λ_{max} = 525 nm) were used as a light source for photobleaching experiments at 0.7 mW/cm^2 intensity. The absorption spectra of the photocatalysts overlayed with the emission spectra of the LED lights used in this study can be found in **Figure S1**. While it is evident that the photocatalysts have differing ranges of absorbance and that the LED emission range does not equally overlap with each photocatalyst, commercially available 525 nm green LED lights are commonly used for each catalyst and avoid the requirement for expensive lasers.[32]

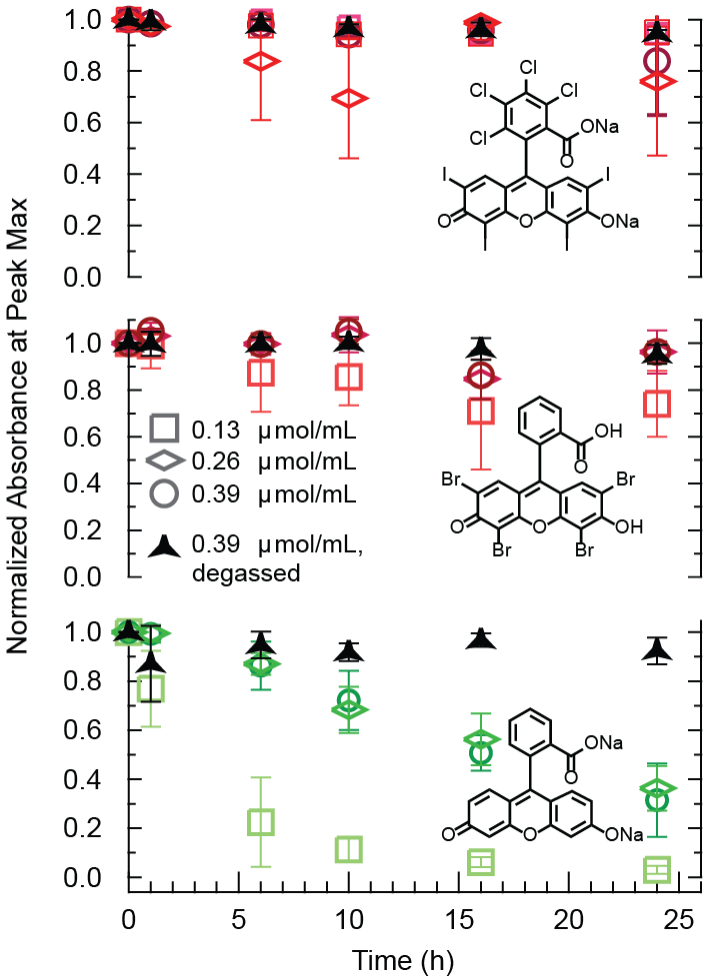

Figure 1. Xanthene dye photobleaching in DMSO exposed to green LED (525 nm) lights in a light bath under different concentrations and conditions as indicated by declines in absorbance with UV-Vis spectroscopy. Rose Bengal (top), Eosin Y (middle) and Fluorescein sodium salt (bottom) are shown.

Figure 1 shows the photobleaching of Rose Bengal (top), Eosin Y (center), and fluorescein (bottom) as a function of time. Both the effects of concentration as well as the presence of

oxygen were investigated. The concentration of photocatalysts (in DMSO) was chosen based on previously reported catalyst loadings for Eosin Y in PET-RAFT polymerization.[26]

For Eosin Y at 0.39 μmol/mL and 0.26 μmol/mL, the absorbance declined to 96% of the original signal after 24 hours of irradiation. Eosin Y at 0.13 μmol/mL showed increased photobleaching, reaching 74% of the original intensity after 24 hours, suggesting a slight concentration dependence for Eosin Y. Verifying the assumption of O_2-tolerance, Eosin Y at 0.39 μmol/mL reached a peak maximum at 95% of the original intensity, suggesting similar behavior to that of the non-degassed sample. Rose Bengal showed a similar trend, reaching 84%, 76%, and 95% (0.39 μmol/mL, 0.26 μmol/mL, and 0.13 μmol/mL, respectively) after 24 hours. The degassed sample of Rose Bengal resulted in 95% retention in signal strength after 24 hours, suggesting that oxygen again did not play a major role in the photobleaching behavior. In contrast to these relatively small effects, concentration and degassing played a more pronounced role in the photobleaching behavior of fluorescein. The 0.39 μmol/mL, 0.26 μmol/mL, and 0.13 μmol/mL samples of fluorescein resulted in 31%, 36%, and 3% retention of the original signal strength, illustrating significantly stronger photobleaching for fluorescein. Unlike the Rose Bengal and Eosin Y samples, degassed fluorescein at 0.39 μmol/mL showed increased resilience to photobleaching, retaining 92% of the signal strength after 24 hours. As such, avoiding oxidation reactions is more relevant in using fluorescein as a photocatalyst. These higher concentrations may result in lower rates of photobleaching as a result of lower light transmission to the center of the reactor vessels (Beer Lambert's law). Reports using Eosin Y for PET-RAFT report concentrations of 0.47 μmol/mL,[26] a similar range as used in this study. At this, and lower, concentrations (0.13 μmol/mL), a transmittance gradient through the reaction vessel is to be expected, with transmitted light from one end of the reaction vial to the other end being 0% for a path length as short as 1.5 cm (see Supporting Information, page 3). This may create a protective effect and portions of Eosin Y photocatalyst do not receive light to undergo photobleaching. Rose Bengal would be expected to follow a similar trend as it also did not appear to exhibit significant degrees of photobleaching within the 24 hour time period. A similar effect may explain the apparent protective effect observed for the homogeneous fluorescein, which underwent the fastest rates of photobleaching at lower concentrations. This appears to show that fluorescein inherently is less photostable than Eosin Y and Rose Bengal. Even though fluorescein has a similar molar extinction coefficient at 525 nm, and therefore

equivalent light penetration, fluorescein still bleached more rapidly than Eosin Y and Rose Bengal.

Photobleaching of xanthene dye heterogeneous photocatalysts

Xanthene dye monolayer synthesis

We investigated the effects of surface-immobilization of xanthene dyes in the form of monolayers. Glass beads of ≤106 μm diameter were prepared with a layer of grafted 3-aminopropyltriethoxysilane (APTES), following an adapted procedure from Teixeira et al. (see SI).[20] The same batch was then separated into three different groups, which were functionalized with fluorescein, Rose Bengal, and Eosin Y via a dicyclohexyl carbodiimide (DCC) coupling. After coupling, the beads were rinsed thoroughly with acetone and dichloromethane (DCM), until the resulting solution appeared clear, and then the beads were further purified using Soxhlet extraction in DCM overnight. Before use, the beads were again stirred and rinsed in DMSO to ensure removal of physiosorbed dyes. **Figure 2** shows the chemical structures of the resulting functionalized beads.

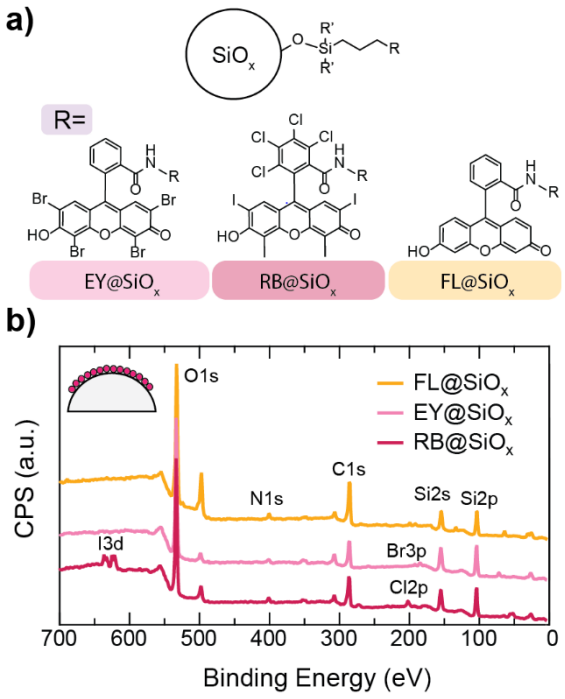

Figure 2. a) Schematic of Xanthene dye photocatalysts directly grafted to glass beads. b) XPS survey spectra after purification of glass beads. The spectra of FL@SiO_x (yellow), EY@SiO_x (pink), RB@SiO_x (purple) notably feature peaks indicating the presence of nitrogen, which is expected from the first step of grafting 3-aminopropyl triethoxysilane. As expected, the EY@SiO_x features a slight peak indicating the presence of bromine, and the RB@SiO_x spectra indicates the presence of both chlorine and iodine. R denotes the xanthene dye groups, while R' denotes the siloxane and silane bonds found at the anchor point.

In the following, the resulting heterogeneous photocatalyst materials will be referred to as EY@SiO_x, FL@SiO_x, and RB@SiO_x for Eosin Y, fluorescein, and Rose Bengal samples, respectively. After grafting, the beads visually appeared in a different color as expected (see **Figure S3**). The FL@SiO_x, EY@SiO_x, and RB@SiO_x appeared in a faint orange, pink, and purple color, respectively. **Figure 2b** shows the photoelectron spectra and surface composition of the beads as determined by X-ray photoelectron spectroscopy (XPS). FL@SiO_x beads were found to have an elemental surface composition of 39.9% carbon, 2.2% nitrogen, 39.1% oxygen, and 18.9% silicon, based on the C1s peak located at 285 eV, the N1s peak at 399 eV the O1s peak located at 532 eV, and the Si2p peak located at 102 eV. EY@SiO_x beads were found to have a surface composition of 40.9% oxygen, 26.8% carbon, 2.2% nitrogen, 1.7% bromine, and 28.3% silicon. RB@SiO_x beads were found to have a surface composition of 40.4% oxygen, 30.8% carbon, 2.0% nitrogen, 0.6% iodine, and 24.3 % silicon. A Na KLL peak was observed in each case at 507.6 eV from the underlying soda lime silica glass.

The detection of nitrogen N1s and silicon (Si2s and Si2p) peaks for each sample suggests a very thin photocatalyst layer, considering an XPS detection depth of approximately 10 nm. Since the only source of nitrogen in these samples is from the APTES used to attach the xanthene dyes, this N1s peak can be used to estimate the amount of coupled dye. For all samples, the theoretical C1s:N1s peak ratio is 24 under the assumption that every amine group is coupled to a dye molecule. The experimentally determined ratios are 18 for FL@SiO_x, 16 for RB@SiO_x, and 12 for EY@SiO_x. This suggests incomplete coupling in each case – likely, in part, due to steric hinderance of the bulky dye molecules and the tendency for APTES to form clustered grafts that would result in residual amine groups. Other carbonaceous contaminations can also rarely be fully excluded in XPS and could further skew the C1s:N1s ratios.

Xanthene dye polymer brush synthesis

To further understand the effects of immobilization and investigate the effects of higher catalyst loadings on surfaces, the xanthene dye photocatalysts were incorporated into polymer brush backbones. This photocatalyst polymer brush approach has been recently studied by our group to produce efficient heterogeneous photocatalysts.[22,33] **Figure 3** shows the resulting heterogeneous polymer brush-based materials and corresponding X-ray photoelectron spectra.

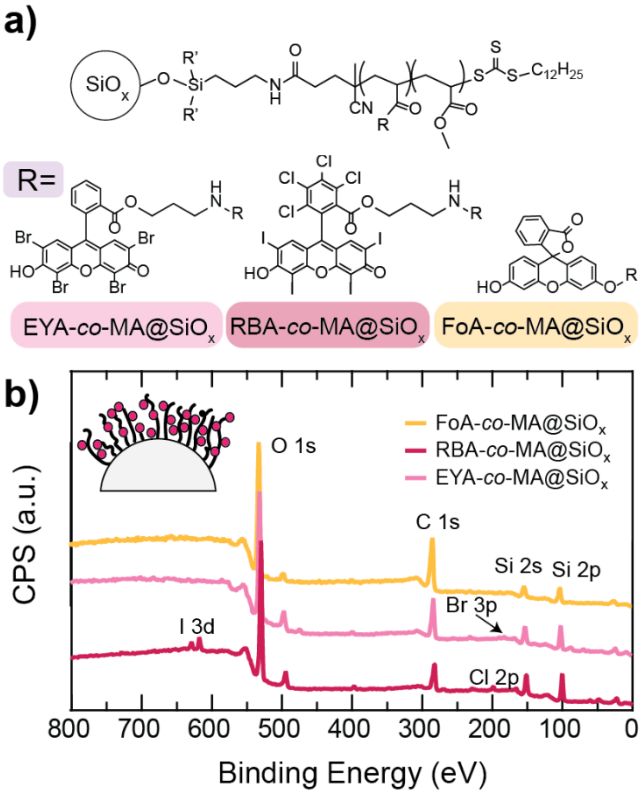

Figure 3. Schematic of chemical structures and XPS spectra of polymer brush-functionalized glass beads. A) Structure of polymer brushes, with the R group representing either Eosin Y or Rose Bengal functionalized with an amine, or fluorescein functionalized in the ortho-position with an acrylate handle. B) XPS survey spectrum for the prepared polymer brush-functionalized beads, FoA-*co*-MA@SiO_x beads (yellow), EYA-*co*-MA@SiO_x (pink), and RBA-*co*-MA@SiO_x (purple). R denotes the xanthene dye groups, while R' denotes the siloxane and silane bonds found at the anchor point.

To synthesize the materials, CDTPA was selected as the RAFT chain transfer agent (CTA), and was grafted to the surface of the glass beads (see **Figure S4**) following our previously published procedure.[22,25,33] Polymer brushes were then grown via surface initiated reversible addition fragmentation chain transfer (SI-RAFT) polymerization (see Supporting Information).

To produce fluorescein-containing polymer brushes, commercially available fluorescein o-acrylate and methyl acrylate were selected. The fluorescein o-acrylate and methyl acrylate were then copolymerized from surface-grafted CDTPA following a previously reported approach by our group to produce FoA-*co*-MA@SiO_x.[33] Analysis of polymers formed in-solution (addition of free CTA) showed a polymer composition of 18 mol % fluorescein-o acrylate, and 82 mol% methyl acrylate. This suggests a slightly higher incorporation of fluorescein than expected at a fluorescein feed ratio of 10 mol%. Surface functionalization of FoA-*co*-MA@SiO_x was confirmed via XPS spectroscopy (see **Figure 3b**) and surface composition was determined as 52% carbon, 34% oxygen, and 14% silicon. The carbon to silicon ratio is 3.8:1 (nearly a two-

fold increase compared to the FL@SiO_x monolayer system) – as expected considering the growth of polymer brushes from the surface resulting in more material loading. A high-resolution carbon C1s scan showed the expected ratio of approximately 2:1:1 for the C-C, C-O, and O=C-O bond environments for the acrylic backbone, with a slightly higher ratio of C-C bonds resulting from the fluorescein moiety (see **Figure S5**).

For Eosin Y and Rose Bengal, transesterification chemistry with pentafluorophenyl acrylate (PFPA)[34] was chosen as an alternative strategy as their monomeric forms are not commercially available. PFPA-*co*-MA copolymers were first grown from surface-grafted CDTPA initiators and then reacted with NH_2-containing xanthene dye photocatalysts to form an amide bond while releasing pentafluorophenol. This method was adapted from Guo et. al, who produced similar polymers using an amine-functionalized Eosin Y to substitute in place of PFPA groups on polymer chains (see **Figure 3a**).[35] Again, a target incorporation of 10 mol% xanthene dye photocatalyst was chosen for EYA-*co*-MA@SiO_x and RBA-*co*-MA@SiO_x to provide sufficient loading of photocatalyst dye as informed by our previous work.[4,22,33] Polymers containing an excess of photocatalytic groups may suffer from reduced efficacy as catalysts may self-quench.[36] Analysis of the freely soluble polymer formed in solution concurrently using ^{1}H-NMR spectroscopy showed 13 mol% PFPA incorporation in 87 mol% MA (see **Figure S6**). Analysis of the freely soluble polymer using Gel Permeation Chromatography (GPC) showed a molecular weight of M_n=14,700 g/mol, M_w = 19,300 g/mol and a dispersity of $Đ$ = 1.31 (see **Figure S7**). After substitution with the xanthene dye photocatalysts, XPS spectroscopy was used to confirm that the characteristic F1s peak from the PFPA had disappeared for both EYA-*co*-MA@SiO_x and RBA-*co*-MA@SiO_x samples (see **Figure S8**). The color of the beads again appeared characteristic of the xanthene dyes (see **Figure S9**). The survey spectra collected for the polymer-brush functionalized beads all indicated a higher incidence of carbon on the surfaces, with C1s peaks increasing from the polymer backbones. The EYA-*co*-MA@SiO_x samples featured 38% oxygen, 1% nitrogen, 20% silicon, 0.2% bromine, and 40% carbon. The carbon-to-silicon ratio was determined as 1.98:1, representing the expected increase in carbon content compared to the EY@SiO_x system. The relativley low abundance of bromine likely results from its volatility under X-ray radiation. The RBA-*co*-MA@SiO_x system was found to have a surface composition of 42% oxygen, 31% carbon, 1% nitrogen, 0.3% iodine, 24% silicon, and 1% chlorine. Iodine and chlorine are both indicative of the presence of Rose Bengal. High resolution C1s photoelectron spectra were also indicative

of characteristic acrylate and acrylamide polymer backbones (see **Figure S5**) and the resulting functionalized beads appeared in a distinctive purple color, indicative of Rose Bengal (see **Figure S9**).

Solid supported xanthene stability against photobleaching

To investigate the stability of xanthene dyes grafted to beads, 1 g of FL@SiO_x, EY@SiO_x, or RB@SiO_x were placed into a vial with 2 mL of DMSO and irradiated under stirring. This approach was chosen to represent a typical experimental setup (and scale) for reported syntheses using heterogeneous organic photocatalysts.[21] The beads were then measured at predefined time intervals using diffuse reflectance (DR) UV-Vis spectroscopy to measure the change in Kubelka-Munk units, which model the likelihood of absorbance.[37] Representative UV-Vis DR spectra for the solid samples may be found in the Supporting Information (see **Figure S10**). The spectra indicate small shifts in the λ_{max} compared to the homogeneous samples, with the largest exception being the FoA-*co*-MA@SiO_x sample, which features a λ_{max} at 436 nm as a result of the free acid form of the fluorescein being the predominant form as opposed to the sodium salt version of fluorescein. For all samples, a significant decrease with time was observed over a 6-hour timespan (see **Figure 4a**).

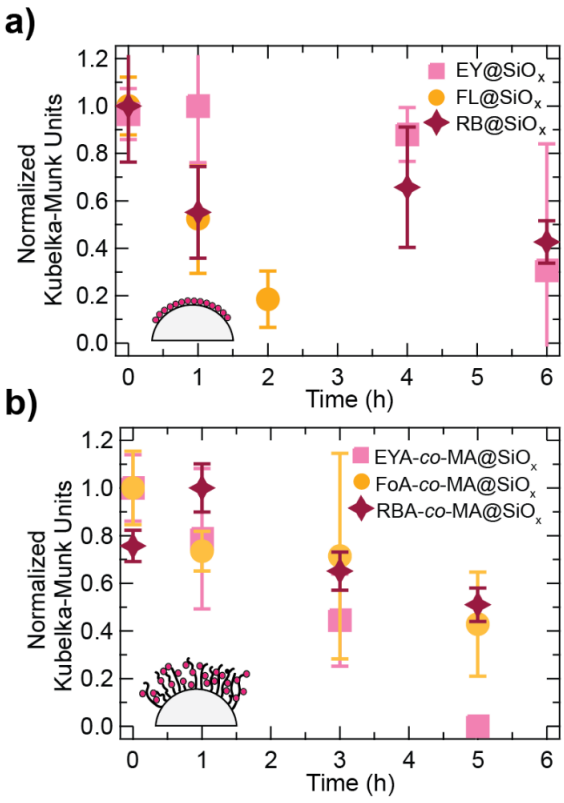

Figure 4. Observed changes Kubelka-Munk units obtained from DR UV-Vis spectroscopy for photocatalyst-immobilized SiO_x samples (1 g of functionalized beads in 2 mL of DMSO and under green LED light and an

environment containing air). a) Kubelka-Munk signal decline for EY@SiO_x, FL@SiO_x and RB@SiO_x samples with time. b) Polymer-brush functionalized beads with Rose Bengal, Fluorescein, and Eosin Y.

As in xanthene dye small molecule solution studies (see **Figure 1**), the fluorescein-based heterogenous catalysts exhibited the most pronounced photobleaching. Nearly 80% of the initial intensity is lost within the first 2 hours of light exposure. The EY@SiO_x, system showed a slight increase in signal after 1 hour, potentially related to an inhibition period of catalyst quenching with oxygen, and then declined to nearly 30% of the original signal strength after 6 hours. The RB@SiO_x, sample showed a more immediate decline, reaching 43% of the original signal strength after 6 hours of exposure to light. Notably, catalyst leaching was observed in each case. To ensure that signal decreases were not solely a result of dye leaching, samples of the solution were tested with UV-Vis and leaching amounts were determined with a calibration curve (see **Figure S11**) to estimate the amount of leached photocatalysts. APTES grafting densities in literature using toluene solvent on silica substrates typically are reported at about 1.3 molecule/nm^2,[38,39] and we may estimate the total grafted amount of Eosin Y using this density, using an average diameter of 76 μm obtained from previous analysis of the bead size,[22] and assuming a full reaction of Eosin Y with the surface-amine groups. Before each measurement, the DMSO solution was extracted from the beads and was analyzed. Time points collected for EY@SiO_x indicated a leaching of Eosin Y at 150 ng after 1 hour and 410 ng at 6 hours. Using the above estimation, this would only explain a loss of 0.2 wt% and 0.7 wt% of the grafted Eosin Y, respectivley. Since the DMSO was replenished after each measurement, an increase in the leaching amount observed indicates potential degrafting, which may take place as a result of the hygroscopic nature of DMSO and the silane groups being susceptible to hydrolysis.[40]

The photocatalyst polymer brush-functionalized beads were also investigated using DR UV-Vis (see **Figure 4b**). In contrast to the monolayer approach, Eosin Y polymer brush beads photobleached more rapidly and characteristic signals were no longer apparent after a 5 hour time period. The residual solution was analyzed with UV-Vis for degrafted polymer chains, showing that 839 ng leached within the first hour, and 37 ng were leached in the last two hours. Using an estimated 1.3 molecules/nm^2 grafting of CDTPA RAFT agent, this would only explain a loss of 0.7 wt% and 0.03 wt% of the Eosin Y contained in the polymer chains. While the largest degree of leaching occured at the beginning of the study, the observed decline in Kubelka-Munk units appeared linear. This suggests that the polymer leaching/degrafting is not

solely responsible for the observed decline, and that photobleaching may explain the majority of the signal decline.

The samples were also studied with fluorescence microscopy to further investigate the fluorescence signal decline over time. Samples were prepared by placing a small amount of beads immersed in DMSO onto a glass microscope slide. The photocatalyst-functionalized beads were then covered with a cover slip that was taped into place to minimize DMSO evaporation and samples were irradiated using green light (λ_{max} = 549 nm, 5 μW/cm^2) continuously for 5 hours (see **Figure S12** and **Figure S13**). Fluorescence fading is a common imaging approach in biological applications, with a decline in fluorescence over time directly related to photobleaching.[41]

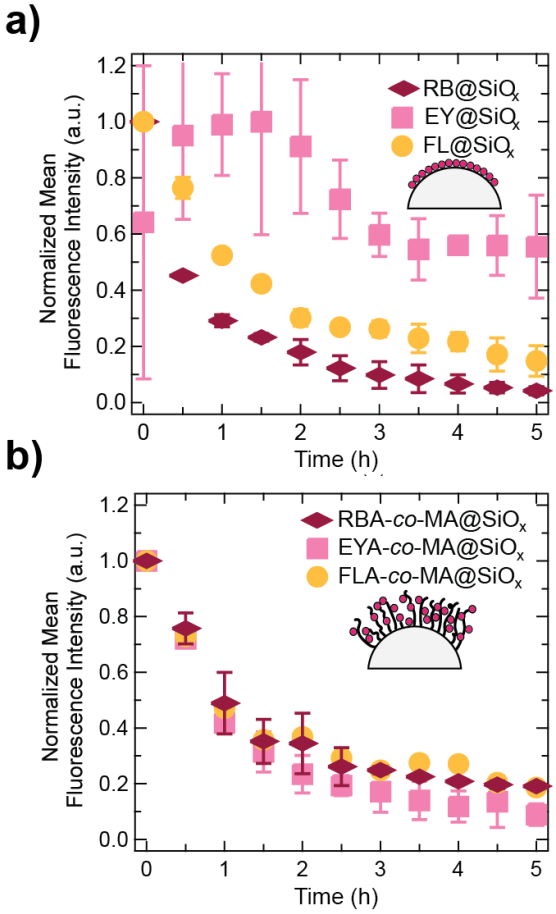

Figure 5. Fluorescence decline obtained through fluorescence microscopy. Samples were irradiated continuously with green light from the microscope's equipped mercury arc lamp. a) Photobleaching of Xanthene dyes grafted to surfaces through coupling with surface-amine groups. b) Photobleaching of Xanthene dyes incorporated into polymer brushes tethered to glass surfaces.

Fluorescence microscopy studies indicated a more rapid rate of photobleaching than was observed for the homogeneous dye photocatalysts. All samples declined to < 25% of the

original intensity within 5 hours. Only EY@SiO_x remained above 50% (see **Figure 5a**). Interestingly, the EY@SiO_x samples appeared to increase in signal intensity for the first hour of light exposure. Fluorescent intensity increases such as this may be caused by aggregation of molecules[42] or perhaps some reduction in self-quenching as degrafting occurs. After the first hour and a half, the samples showed a decline in fluorescence, with a stabilization occuring after 3 hours at 56% of the maximum observed value. The polymer brush-based samples showed a similar pattern (see **Figure 5b**). However, the EYA-*co*-MA@SiO_x samples showed an immediate decline in signal and, after 5 hours, the signal was only 9% of the original intensity – compared to the 56% signal obtained from the directly grafted EY@SiO_x. In contrast, RBA-*co*-MA@SiO_x appeared slightly more resilient than the RB@SiO_x sample, with 72% signal retained for the polymer brushes and 45% signal retained for the directly grafted sample by the end of the study. However, after 5 hours, the RBA-*co*-MA@SiO_x retained only 19% and the RB@SiO_x retained only 4% of the original signal indicating that both samples were still susceptible to photobleaching. Overall, the FL@SiO_x samples appeared very similar to the FoA-*co*-MA@SiO_x samples. The directly-grafted FL@SiO_x sample reached 76% of the original signal strength while the polymer brush samples reached 73% after the first half hour. After 5 hours, the FL@SiO_x reached 15% while the FoA-*co*-MA@SiO_x reached 19%, still showing only minor differences.

We hypothesize that photocatalyst polymer brushes swollen in good solvent could reduce photobleaching resulting from dye-dye interactions. Polymer brushes may also protect the silane bonds from hydrolysis and therefore may result in more surface-stable functionalized surfaces.[43] However, fluorescence microscopy and UV-Vis spectroscopy indicated that the polymer brushes did not provide substantial protection from photobleaching compared to the directly grafted photocatalyst dyes. The results from the fluorescence microscopy studies seem to indicate that Rose Bengal benefits from higher catalyst loadings, while Eosin Y may be more sensitive to photobleaching from dye-dye interactions. Another important consideration when comparing the photobleaching of the two dyes is that Rose Bengal has been demonstrated to be a superior photosensitizer to Eosin Y,[31] so photobleaching resulting from the presence of oxygen may be reduced in the case of Rose Bengal as DMSO is more rapidly converted to dimethyl sulfone.

Removal of oxygen has been shown to increase the stability of fluorescein in aqueous systems, where degassed solutions showed higher photostability.[12] Simulations by Song et. al. modeled

the bleaching behavior based on the relative ratios of fluorescein and oxygen in water, with a fluorescein to oxygen ratio of 1:2.5 resulting in photobleaching from oxygen being the dominant factor while a fluorescein to oxygen ratio of 40:1 results in photobleaching from fluorescein-to-fluorescein reactions being dominant.[12] These results suggest that surface immobilization can impact the photobleaching behavior of xanthene dyes, since the nature of surface immobilization will result in higher local concentrations of catalyst. The results obtained in **Figure 4** and **Figure 5** indicate potential consequences of surface grafting, because in each case, each species faded substantially more than the homogeneous analogues.

Additionally, in the case of systems created via the immobilization of APTES onto glass, trace amounts of moisture can result in the clustering of APTES as it polymerizes on the surface of SiO_x.[38] It is feasible that the grafting of xanthene dyes to silica surfaces can increase the incidence of dye-dye bleaching, as coupled dyes will have limited movement resulting from the relatively short (3 carbon) linkage from the dye to the Si-anchor point. In contrast, polymer brushes can reduce dye-dye bleaching (compared to the directly grafted dyes) because polymer brushes allow for varied incorporations of photocatalysts. This modifies photocatalyst density within the brush and the relative spacing of dyes upon swelling in different solvents. Tas et. al. observed decreased fluorescence in polymer brushes in a collapsed state from exposure to water as a solvent compared to an 80/20 ratio of isopropanol to water.[44]

Dong et. al. found in their studies of Rhodamine 6G and gold nanoparticle systems that larger ratios of radiative decay (energy emission from the dye in the form of fluorescence) to non-radiative decay (energy emission in the form of heat or energy transfer to another molecule) seem to result in slower rates of photobleaching over time.[45] And therefore fluorescence lifetimes and fluorescence resonance energy transfer (FRET)[46] are interesting parameters to consider for photocatalytic materials. Fluorescence lifetime refers to the average time between the excitation of the dye and the emission of a photon in the form of fluorescence.[47] For the case of the polymer brush systems herein, the dye molecules are able to undergo fluorescence, and non-radiative decay may take place in the form of homo-FRET, which describes the transfer of energy from fluorophore to the same species of fluorophore.[48] However, in the case of homo-FRET, a decrease in fluorescence lifetime is not expected.[48] Fluorescence lifetime imaging microscopy was performed on the samples (see **Figure S14**). For the case of the Eosin Y systems studied, a fluorescence lifetime (τ) of ns ± 0.00, 3.13 ns ± 0.07, and 3.16 ns ± 0.01 was observed for the homogeneous Eosin Y, EY@SiO_x, and EYA-*co*-

MA@SiO_x systems in DMSO, respectivley. These results indicate no major changes in fluorescence lifetimes, as expected for homo-FRET.

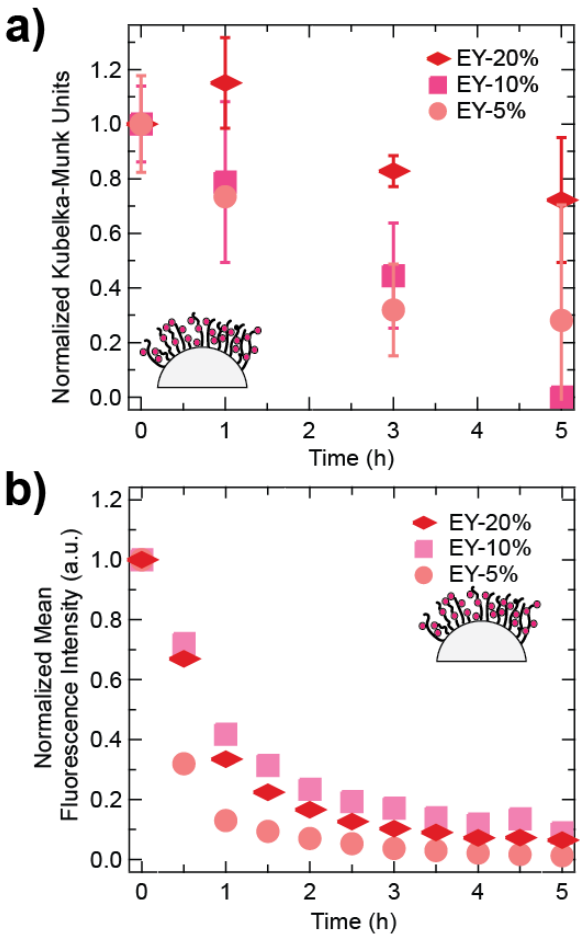

Figure 6. Fluorescence decline obtained through DR UV-Vis fluorescence microscopy for EYA-*co*-MA@SiO_x polymer brushes containing varied loadings of Eosin Y. The EY-10% traces are reproduced from **Figures 4b and 5b** a) Photobleaching measured with DR UV-Vis with exposure to green LEDs in light bath (0.7mW/cm^2,λ_{max}=525 nm). b) obleaching of samples studied with fluorescence microscopy (λ_{max} = 549 nm, 5 µW/cm^2).

To investigate the relative spacing of dyes and their possible effect on photobleaching and energy transfer, further studies altered the relative incorporation of Eosin Y in the EYA-*co*-MA@SiO_x polymer brush systems. Relative molar feed ratios of 5%, 10%, and 20% of pentafluorophenyl acrylate were added into the polymerization solutions and Eosin Y-NH_2 was substituted to create samples with different relative loadings, referred to as EY-5%, EY-10%, and EY-20%. ^{1}H NMR and ^{19}F NMR analysis determined 6%, 13%, and 23% molar loadings of PFPA compared to MA. UV-Vis DR and fluorescence microscopy experiments were performed as described previously. Results indicate that under more mild light irradiation with the LED light bath at λ_{max}= 525 nm and 0.7 mW/cm^2 irradiation, the 20% sample appears to be

the most stable, while the 10% and 5% samples fade more rapidly, with each showing a signal strength below 30% of the starting signal by the 5th hour (see **Figure 6a**). In contrast, the 20% sample remained above 70% of the original signal strength for the duration of the experiment. Interestingly, a different trend was observed for the fluorescence microscopy studies (see **Figure 6b**), which used the microscope's own mercury arc lamp (λ_{max} = 549 nm, 5 μW/cm^2). In this case, the 20% sample bleached similarly to the 10% sample. This indicates a potential non-linear relationship between the degradation rate and the incorporation of photocatalyst contained in the polymer brush. A potential explanation could be that the increased light intensity seen in the microscopy studies results in more dye-dye interactions that lead to photobleaching more quickly in the EY-20% sample than the EY-10% sample.

While the results in these studies do not appear to indicate that surface-immobilization provides increased photostability compared to homogeneous settings, it is noteworthy that there exist several studies of surface-immobilized xanthene dye photocatalysts on silica or glass supports. Many of these studies show not only good catalytic functioning, but also good recyclability over prolonged periods of irradiation.[18,20,22,49,50] This suggests that the resilience of photocatalysts to photobleaching is significantly impacted by the reactants and different reaction systems resulting in different stability. To test this hypothesis, the EYA-*co*-MA@SiO$_x$ at a 10% loading of EY (also refered to as EY-10%) beads were selected since they showed a loss of the characteristic Eosin Y signal after 5 hours. Eosin Y has been demonstrated to be an effective photocatalyst for PET-RAFT polymerization with the chain transfer agent (CTA) 4-cyano-4-(phenylcarbonothioylthio)pentanoic acid (CPADB).[51] In addition, tertiary amines are known to aid in the oxygen tolerance of these systems as energy transfers from Eosin Y to oxygen are not favorable to promote polymerization.[52] Therefore, following the same procedure described previously, 1 g of EYA-*co*-MA@SiO$_x$ beads were placed into a vial with 2 mL of DMSO and stirred vigourously for 5 hours under green LEDs in the presence of 13.1 mg CPADB and 4.6 μL triethyl amine. Afterwards, the beads were rinsed thoroughly with DMSO and measured using DR UV-Vis to analyze photobleaching behavior (see **Figure 7**).

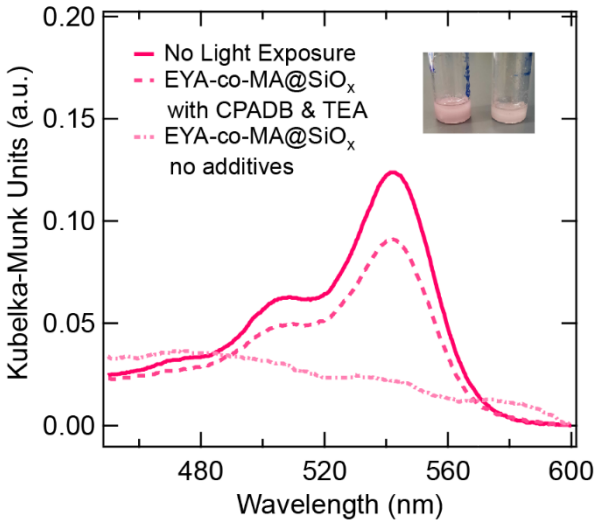

Figure 7. DR UV-Vis spectrum of the EYA-*co*-MA@SiO_x (at a 10% loading of EY, EY-10%) unbleached, placed in the presence of 4-Cyano-4-(phenylcarbonothioylthio)pentanoic acid (CPADB) and triethyl amine (TEA) in DMSO under conditions used to catalyze PET-RAFT, and EYA-*co*-MA@SiO_x in DMSO with no additives. The insert (left) shows the pink color retained for the beads in the presence of CPADB and TEA after washing, while (right) shows the EYA-*co*-MA@SiO_x without these additives under the same green LED light irradiation for 5 hours.

The results obtained confirmed our hypothesis that the photobleaching of Eosin Y polymer brushes may be reduced when in the presence of CTA and a tertiary amine. While the EYA-*co*-MA@SiO_x placed in DMSO and irradiated with green light no longer showed the characteristic Eosin Y peak, the EYA-*co*-MA@SiO_x irradiated with green light in the presence of CTA and tertiary amine retained 74% of the signal observed for the unbleached sample. Encouragingly, these results suggest that while heterogeneous photocatalysts may initially demonstrate relatively low photostability compared to the required reaction times, reaction conditions may be altered such that energy or electron transfers are promoted, and this appears to increase the photocatalyst stability.

Conclusions

In conclusion, the photobleaching behavior of fluorescein, Eosin Y, and Rose Bengal was studied in homogeneous solution, when grafted to glass beads through APTES coupling, and when incorporated into polymer brushes as comonomers. The homogeneous solutions resulted in the slowest rates of photobleaching, with fluorescein showing the most rapid photobleaching behavior that displayed both concentration and oxygen dependence. Surface immobilization appeared to reduce the photostability of the xanthene dyes in all cases, but Eosin Y appeared the most stable. When incorporated into polymer brushes, Rose Bengal showed increased resilience compared to the monolayer system, while Eosin Y showed decreased longevity. This

may be the result of different sensitivities to dye-dye bleaching. Fluorescein in both cases showed similar bleaching rates. Lastly, the photostability of EYA-*co*-MA@SiO_x was investigated in the presence of PET-RAFT conditions, and the stability was improved. Overall, these findings indicate that the immobilization strategies as well as local concentrations of catalyst dyes impact the photostability.

Acknowledgements

The authors thank Dr. Gina Noh and Winters Guo for their assistance in UV-Vis spectroscopy and acknowledge NSF CBET Award # 2143628 for financial support.

Received: ((will be filled in by the editorial staff))

Revised: ((will be filled in by the editorial staff))

Published online: ((will be filled in by the editorial staff))

References

[1] R. Ameta, M.S. Solanki, S. Benjamin, S.C. Ameta, *Adv. Oxid. Process. Wastewater Treat. Emerg. Green Chem. Technol.*, **2018**, 135–175.

[2] R.C. McAtee, E.J. McClain, C.R.J. Stephenson, *Trends Chem.*, **2019**, *1*, 111–125.

[3] N.A. Romero, D.A. Nicewicz, *Chem. Rev.*, **2016**, *116*, 10075–10166.

[4] J.D. Bell, J.A. Murphy, *Chem. Soc. Rev.*, **2021**, *50*, 9540–9685.

[5] K. Teegardin, J.I. Day, J. Chan, J. Weaver, *Org. Process Res. Dev.*, **2016**, *20*, 1156–1163.

[6] C. Wu, N. Corrigan, C.H. Lim, K. Jung, J. Zhu, G. Miyake, J. Xu, C. Boyer, *Macromolecules*., **2019**, *52*, 236–248.

[7] C. Wu, N. Corrigan, C.H. Lim, W. Liu, G. Miyake, C. Boyer, *Chem. Rev.*, **2022**, *122*, 5476–5518.

[8] N. Bono, F. Ponti, C. Punta, G. Candiani, *Materials (Basel).*, **2021**, *14*, 1–20.

[9] B. Li, Y. Hu, Z. Shen, Z. Ji, L. Yao, S. Zhang, Y. Zou, D. Tang, Y. Qing, S. Wang, G. Zhao, X. Wang, *ACS ES&T Eng.*, **2021**, *1*, 947–964.

[10] Y. Urano, M. Kamiya, K. Kanda, T. Ueno, K. Hirose, T. Nagano, *J. Am. Chem. Soc.*, **2005**, *127*, 4888–4894.

[11] O. Kravchenko, T.C. Sutherland, B. Heyne, *Photochem. Photobiol.*, **2022**, *98*, 49–56.

[12] L. Song, E.J. Hennink, I.T. Young, H.J. Tanke, *Biophys. J.*, **1995**, *68*, 2588.

[13] L. Song, C.A.G.O. Varma, J.W. Verhoeven, H.J. Tanke, *Biophys. J.*, **1996**, *70*, 2959–2968.

[14] L.S. Herculano, L.C. Malacarne, V.S. Zanuto, G.V.B. Lukasievicz, O.A. Capeloto, N.G.C. Astrath, *J. Phys. Chem. B*., **2013**, *117*, 1932–1937.

[15] S. Gisbertz, B. Pieber, C. Reviews, *ChemPhotoChem*., **2020**, *4*, 456–475.

[16] A.O. Ibhadon, P. Fitzpatrick, *Catal. 2013, Vol. 3, Pages 189-218*., **2013**, *3*, 189–218.

[17] Y. Wang, X. Wang, M. Antonietti, *Angew. Chemie Int. Ed.*, **2012**, *51*, 68–89.

[18] S. Shanmugam, S. Xu, N.N.M. Adnan, C. Boyer, *Macromolecules*., **2018**, *51*, 779–790.

[19] G.J. Barbante, T.D. Ashton, E.H. Doeven, F.M. Pfeffer, D.J.D. Wilson, L.C. Henderson, P.S. Francis, *ChemCatChem*., **2015**, *7*, 1655–1658.

[20] R.I. Teixeira, N.C. De Lucas, S.J. Garden, A.E. Lanterna, J.C. Scaiano, *Catal. Sci. Technol.*, **2020**, *10*, 1273–1280.

[21] K. Bell, S. Freeburne, A. Wolford, C.W. Pester, *Polym. Chem.*, **2022**, *13*, 6120–6126.

[22] K. Bell, S. Freeburne, M. Fromel, H.J. Oh, C.W. Pester, *J. Polym. Sci.*, **2021**, *59*, 2844–2853.

[23] J.C.S. Terra, A. Desgranges, Z. Amara, A. Moores, *Catal. Today*., **2023**, *407*, 52–58.

[24] Z. Li, H. Song, R. Guo, M. Zuo, C. Hou, S. Sun, X. He, Z. Sun, W. Chu, *Green Chem.*, **2019**, *21*, 3602–3605.

[25] K. Bell, Y. Guo, S. Barker, S.H. Kim, C.W. Pester, *Polym. Chem.*, **2023**, *14*, 2662–2669.

[26] J. Xu, S. Shanmugam, H.T. Duong, C. Boyer, *Polym. Chem.*, **2015**, *6*, 5615–5624.

[27] C. Bian, Y.N. Zhou, J.K. Guo, Z.H. Luo, *Macromolecules*., **2018**, *51*, 2367–2376.

[28] Y. Zhang, X. Yue, C. Liang, J. Zhao, W. Yu, P. Zhang, *Tetrahedron Lett.*, **2021**, *80*, 153321.

[29] S. Sharma, A. Sharma, *Org. Biomol. Chem.*, **2019**, *17*, 4384–4405.

[30] N. Corrigan, D. Rosli, J.W.J. Jones, J. Xu, C. Boyer, *Macromolecules*., **2016**, *49*, 6779–6789.

[31] L. V Lutkus, S.S. Rickenbach, T.M. Mccormick, **2019**,.

[32] C.R. Horn, S. Gremetz, *Beilstein J. Org. Chem.*, **2020**, *16*, 871.

[33] K. Bell, S. Freeburne, A. Wolford, C.W. Pester, *Polym. Chem.*, **2022**, *13*, 6120–6126.

[34] H. Son, Y. Jang, J. Koo, J.S. Lee, P. Theato, K. Char, *Polym. J. 2016 484*., **2016**, *48*, 487–495.

[35] W.L. Guo, Y. Zhou, B. Duan, W.F. Wei, C. Chen, X. Li, T. Cai, *Chem. Eng. J.*, **2022**, *429*, 132120.

[36] J.J. Nichols, P.E. King-Smith, E.A. Hinel, M. Thangavelu, K.K. Nichols, *Invest. Ophthalmol. Vis. Sci.*, **2012**, *53*, 5426–5432.

[37] V. Džimbeg-Malčić, Ž. Barbarić-Mikočević, K. Itrić, n.d.,.

[38] R.M. Pasternack, S.R. Amy, Y.J. Chabal, *Langmuir*., **2008**, *24*, 12963–12971.

[39] B. Qiao, T.-J. Wang, H. Gao, Y. Jin, *Appl. Surf. Sci.*, **2015**, *351*, 646–654.

[40] E.A. Smith, W. Chen, *Langmuir*., **2008**, *24*, 12405–12409.

[41] N.B. Vicente, J.E. Diaz Zamboni, J.F. Adur, E. V. Paravani, V.H. Casco, *J. Phys. Conf. Ser.*, **2007**, *90*,.

[42] A. Kitamura, M. Kinjo, *Biophys. Physicobiology*., **2018**, *15*, 1.

[43] Z. Ding, C. Chen, Y. Yu, S. de Beer, *J. Mater. Chem. B*., **2022**, *10*, 2430–2443.

[44] S. Tas, M. Kopec, R. van der Pol, M. Cirelli, I. de Vries, D.A. Bölükbas, K. Tempelman, N.E. Benes, M.A. Hempenius, G.J. Vancso, S. de Beer, *Macromol. Chem. Phys.*, **2019**, *220*, 1800537.

[45] L. Dong, F. Ye, J. Hu, S. Popov, A.T. Friberg, M. Muhammed, *J. Eur. Opt. Soc. Publ.*, **2011**, *6*, 11019.

[46] R.B. Sekar, A. Periasamy, *J. Cell Biol.*, **2003**, *160*, 629.

[47] R. Yasuda, *Neurophotonics Biomed. Spectrosc.*, **2019**, 53–64.

[48] E.R. Lampugnani, R.H. Wink, S. Persson, M. Somssich, *CRC. Crit. Rev. Plant Sci.*, **2018**, *37*, 308–334.

[49] S.M. Soria-Castro, B. Lebeau, M. Cormier, S. Neunlist, T.J. Daou, J.P. Goddard, *European J. Org. Chem.*, **2020**, *2020*, 1572–1578.

[50] N. Body, C. Lefebvre, P. Eloy, T. Haynes, S. Hermans, O. Riant, *J. Photochem. Photobiol. A Chem.*, **2023**, *440*, 114648.

[51] J. Xu, S. Shanmugam, H.T. Duong, C. Boyer, *Polym. Chem.*, **2015**, *6*, 5615–5624.

[52] B. Nomeir, O. Fabre, K. Ferji, *Macromolecules*., **2019**, *52*, 6898–6903.

ABSTRACT

The photobleaching behavior of xanthene dye photocatalysts is investigated. Rose Bengal, Eosin Y, and fluorescein are studied in solution, when grafted to glass beads, and when incorporated into polymer brushes that are tethered to glass beads. Photobleaching was investigated with UV-Vis, diffuse reflectance UV-Vis (DR UV-VIS), and with fluorescence microscopy. The homogeneous photocatalysts exhibited the highest photostability, while the grafted systems appeared to fade more rapidly. Notably, heterogenization appeared to have different effects based on the photocatalyst system.

*Sarah Freeburne, Jessica L. Sacco, Esther W. Gomez, Christian W. Pester**

tobleaching Behavior of Xanthene Dye Photocatalysts